DOI 10.5162/sensor2015/E8.2

Nanostructured WO_3 Semiconductor Gas Sensor for Selective Detection of Naphthalene

Martin Leidinger[1], Joni Huotari[2], Tilman Sauerwald[1], Jyrki Lappalainen[2], Andreas Schütze[1]
[1]Saarland University, Campus A5 1, 66123 Saarbrücken, Germany,
m.leidinger@lmt.uni-saarland.de
[2]Microelectronics and Materials Physics Laboratories, University of Oulu,
P.O. Box 4500, FIN-90014 Oulu, Finland

Abstract

Pulsed laser deposition at room temperature was used to prepare WO_3 layers on MEMS micro heater platforms obtaining porous layers of nanoparticles and nanoparticle agglomerates. The layer structure and the related gas sensing properties were shown to be highly dependent on the deposition parameters, especially the oxygen pressure. At an oxygen pressure of 0.2 mbar the formation of ε-phase WO_3 was found resulting in an increased sensitivity of the sensor material.
The gas sensing performance was determined by exposing the WO_3 sensor devices to volatile organic compounds (benzene, formaldehyde, naphthalene) at ppb level concentrations and ethanol background at ppm level concentrations. The sensors were operated in temperature cycled operation; the signal processing was performed using linear discriminant analysis based on shape features extracted from the conductance signals. Both tested sensor layers showed high sensitivity and selectivity to naphthalene compared to the other test gases. The sensor layer deposited at higher oxygen partial pressure performed better for discriminating the gases and naphthalene concentrations. With this sensor, 1 ppb of naphthalene could be detected in a 1 ppm ethanol background with very high reliability. Furthermore a discrimination of 5 ppb of naphthalene from lower concentrations for quantification purposes was possible.

Key words: Pulsed laser deposition, WO_3, indoor air quality, gas sensor, temperature cycled operation

Introduction

The quality of indoor air is deteriorated by the presence of hazardous volatile organic compounds (VOCs) like benzene, formaldehyde and naphthalene [1]. For naphthalene, the World Health Organization (WHO) guidelines suggest values below 0.01 mg/m³ (1.88 ppb) [1]. We found that metal oxide semiconductor (MOS) gas sensors using tungsten trioxide (WO_3) as gas sensitive material prepared by pulsed laser deposition respond to naphthalene in this concentration range with high selectivity compared to other gases, e.g. ethanol.
Pulsed laser deposition (PLD) is a very versatile method for depositing thin films and nanostructured layers from various materials, e.g. for gas sensing purposes [2,3]. When using nanosecond laser PLD, as in this study, with a high oxygen partial pressure in the deposition chamber, nanoparticle formation starts during the deposition process leading to a highly porous nanostructured layer [4]. These types of layers are very suitable for gas sensing purposes because of their high specific surface area. With this method, WO_3 layers were deposited on MEMS micro heaters to produce gas sensor devices.
Test gas measurements were performed with three VOC target gases in trace concentrations and an interferent gas in a much higher concentration. The sensors were operated in temperature cycled operation (TCO). Signal processing was conducted by multivariate pattern recognition methods, especially Linear Discriminant Analysis (LDA). This method was shown to improve selectivity and sensitivity of various other MOS and GasFET sensors for VOC trace gas detection [5,6,7,8]

Sensor layer deposition

Pulsed laser deposition with a XeCl (λ = 308 nm) laser was used to produce WO_3 layers on commercial micro heater MEMS platforms from a ceramic WO_3 pellet. The laser pulse length was 25 ns and pulse fluence was I = 1.25 J/cm^2. In all depositions the substrate temperature was kept at room temperature (RT) and the O_2 partial pressures were $p(O_2)$ =

0.08 mbar and 0.2 mbar, respectively. Samples were annealed in a furnace at 400 °C for 1 h after deposition.
X-ray diffraction with Bruker D8 Discover and Raman spectroscopy with HORIBA Jobin Yvon LabRAM HR800 were used to study the crystal structure and symmetry of the layers. The morphology of the samples was studied with Veeco Dimension 3100 atomic force microscope (AFM).

Layer characterization

To study the crystal structure of the samples, the grazing incidence diffraction (GID) method of the X-ray diffraction was used to characterize the post-annealed layers. The results are shown in Fig. 1. A clear difference in the crystal structure is evident. The phase composition of layers deposited at $p(O_2)$ = 0.08 mbar is mostly of monoclinic γ-phase of WO_3, but in the samples deposited at $p(O_2)$ = 0.2 mbar, also ferroelectric monoclinic ε-phase of WO_3 is present, emphasized especially by the peaks located at 2θ ≈ 24.1° and 33.3° [9].

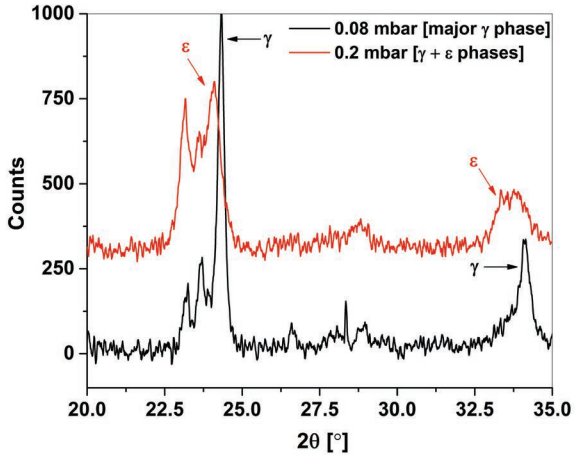

Fig. 1: X-ray diffraction curves of the annealed samples deposited at two different O_2 partial pressures

The crystal symmetry of the nanoparticles was also studied by Raman spectroscopy and the results are shown in Figs. 2 a) and b). In Fig. 2 a), the Raman spectra of the samples immediatly after deposition without any heat treatment are shown, and in Fig. 2 b), the spectra of the layers after post-annealing at 400 °C are presented. An interesting property of the deposition process can be identified in the non-annealed samples (Fig. 2a). When the O_2 partial pressure is 0.08 mbar, the samples seem to be in amorphous state after deposition, but when the O_2 pressure is 0.2 mbar, some crystallization is already evident during the deposition process at RT, even before any heat treatments to the layers. From Fig. 2 b), showing the Raman spectra of the samples after the post-annealing process, it is again evident that the layers deposited at $p(O_2)$ = 0.08 mbar are composed mostly of γ-phase, but the samples deposited at $p(O_2)$ = 0.2 mbar also show the ε-phase in their crystal structure [9].

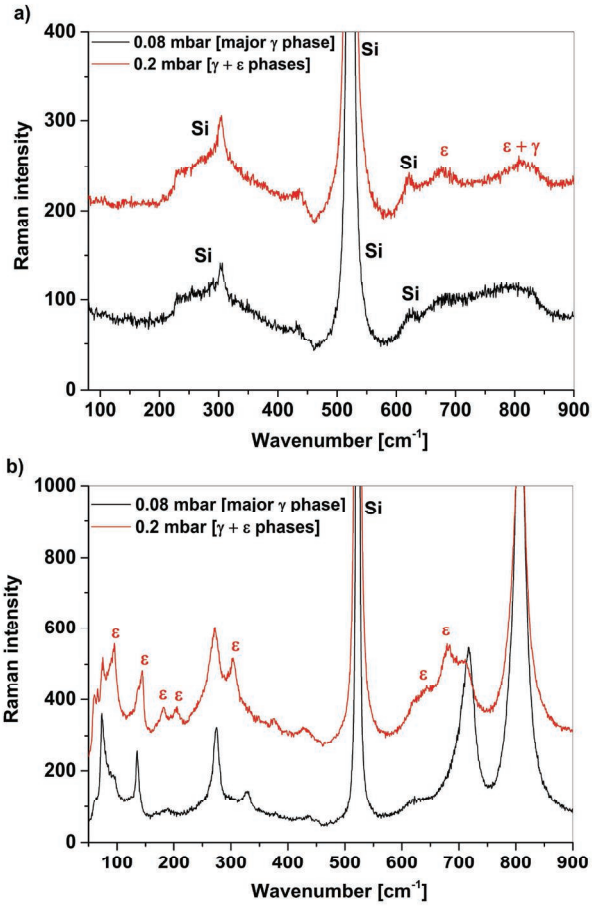

Fig. 2: Raman spectra of the samples deposited at two different O_2 partial pressures a) before any heat treatments, and b) after post-annealing at 400 °C.

Morphologies of the deposited and post-annealed WO_3 samples were studied by atomic force microscopy and the results are shown in Fig. 3. The sample deposited at an O_2 partial pressure of 0.08 mbar consists of small agglomerates of nanoparticles with an average surface roughness of R_q = 5.5 nm. On the other hand, the layer deposited at $p(O_2)$ = 0.2 mbar consists also of small nanoparticles, but agglomerated to bigger clusters. Also, the layer structure is much rougher and more porous than on the samples deposited at 0.08 mbar O_2. The R_q value of the sample in Fig. 3 b) is R_q = 42.2 nm. The average grain size of the samples was determined to be around 30 nm using the Warren-Averbach method for XRD data [10].

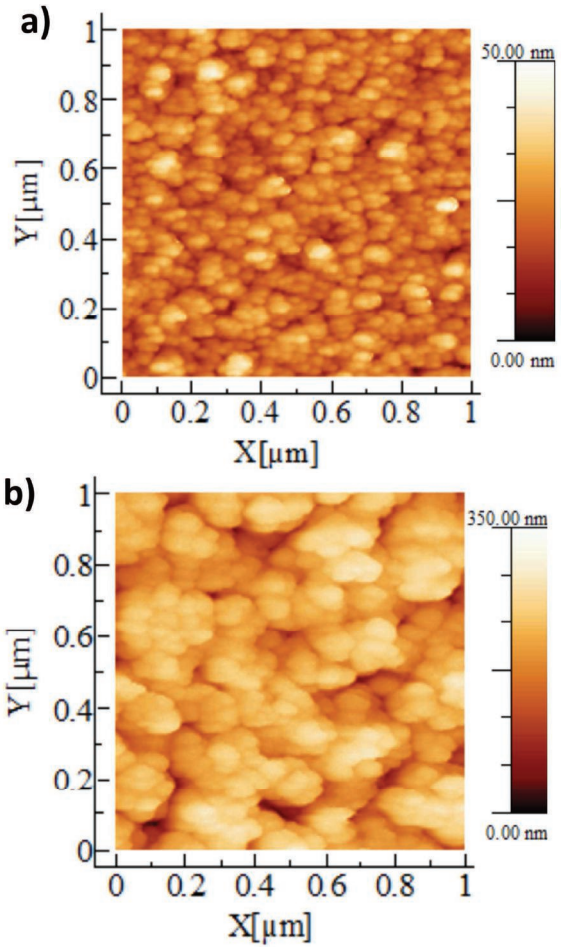

Fig. 3: Atomic force microscopy graphs of the WO_3 layers deposited at O_2 pressure of a) 0.08 mbar, b) 0.2 mbar after annealing at 400 °C

When using 0.2 mbar O_2 partial pressure the layers have a very porous structure consisting of agglomerates of small nanoparticles. On the other hand, the samples deposited at $p(O_2)$ = 0.08 mbar have a smoother surface and they consist of much smaller agglomerates.

Gas measurements

The two prepared gas sensor types were tested with three target VOCs, variable gas humidity and interferent background (ethanol). Each target VOC was applied in three concentrations (Table 1). The medium concentration in each case corresponds to the respective WHO guideline value for indoor air [1]. Each VOC in each concentration was combined with each ethanol and humidity variation resulting in 90 test conditions in total (Table 1).

Gas mixtures were generated using an automated gas mixing system designed specifically for trace gas generation [11].

Table 1: VOC concentrations and variations of background humidity and interferent gas concentration during the test measurement

Gas	**c / ppb**
Formaldehyde	200; 80; 40; 40; 80; 200
Benzene	2.5; 1.5; 0.5; 0.5; 1.5; 2.5
Naphthalene	5; 2; 1; 1; 2; 5

Background	
Relative humidity	30; 50; 70 %
Ethanol	0; 0.5; 1 ppm

The sensors were operated in temperature cycled operation (TCO) in order to increase sensitivity, selectivity and stability of the signals [5,6,7,12]. For operation of the sensor devices and data acquisition, electronics by 3S GmbH (Saarbruecken, Germany) were used. As a temperature cycle, a ramp-up / ramp-down approach was selected (Fig. 4). The temperature of the sensors was increased from 200 °C to 400 °C in 20 s and then reduced to 200 °C in the same time. The sensor signals (Fig. 4) correspond to the conductance of the sensing layers. The two sensor types clearly show different behavior during the temperature cycle, especially during increase of the heater temperature.

A preliminary signal evaluation is performed with the quasi-static sensor signals which are generated by plotting the signal value of a certain point in the TCO cycle, i.e. a certain temperature of the sensor, for each cycle, i.e. over time. Fig. 6 shows a segment of the signal of sensor PLD-2e-1 (0.2 mbar O_2), taken from the point 20 s into each cycle, which is the point of the highest temperature (Fig. 4). The sensor shows a significant response to naphthalene

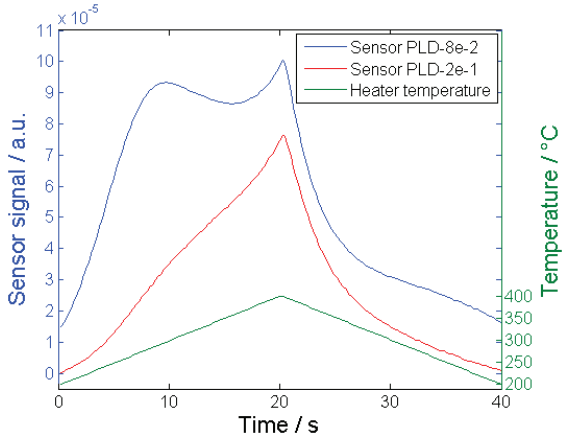

Fig. 4: Visualization of the temperature cycle and corresponding sensor signals of the two different gas sensors

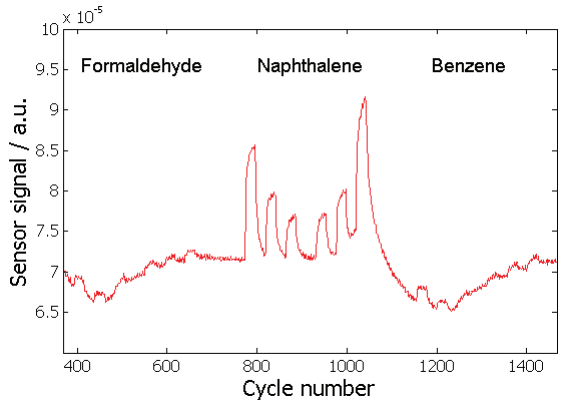

Fig. 6: Segment of the quasi-static sensor signal of sensor PLD-2e-1, during one run of the test VOCs, at 30 %rh and no EtOH background.The chosen point of the signal is 20 s into the TCO cycle

while the responses to formaldehyde and benzene are comparably very low.

The dynamic sensor signal patterns were analyzed using Linear Discriminant Analysis (LDA, [13,14]). As input data for this method, a limited number of features were extracted from the sensor signals in each temperature cycle in the following manner. The cycle was divided into 20 sections of equal length. In each segment the mean value and the slope were calculated and used as features. This generates a feature vector with 40 values for each temperature cycle.

The first LDA discrimination is the separation of the different VOC gases ("Ansatz A1") independent of their concentration, the RH level or the interferent gas concentration. For this, all signal cycles recorded during application of the respective VOC, with all RH levels and ethanol backgrounds, were assigned to the same group. This leads to four groups, i.e. one for each target VOC and one "background" group for the segments of the measurement without the trace gases, i.e. pure air or ethanol only. The results are shown in Fig. 5 for sensor PLD-8e-2 (0.08 mbar O_2 partial pressure during deposition) and in Fig. 7 for sensor PLD-2e-1 (0.2 mbar). For both sensors, the naphthalene group (light blue) is separated from the background group (dark blue) in the first discriminant function, while the other trace VOCs are shifted along the second discriminant function. The naphthalene group is separated much more clearly from the background, especially for sensor PLD-2e-1. To compare the LDA results of the two sensors, the classifications were evaluated using leave-one-out cross validation (LOOCV). This method calculates the LDA parameters using all data sets but one, and then evaluates and classifies the left out data set. This is performed for all TCO data sets. Classification is calculated using the k-nearest-neighbors approach with k = 5. The result for the discrimination of the VOCs is shown in Table 2.

Table 2: LOOCV results for LDA of both sensors, Ansatz A1

Group	Correctly classified data points [%], Ansatz A1	
	PLD-8e-2	PLD-2e-1
Overall	66.4880	71.9185
Background	10.8491	48.5849
Benzene	67.7868	57.8216
Formaldehyde	59.1435	64.5833
Naphthalene	86.2791	99.1860

While classifications of benzene and formaldehyde are poor for both sensors, the amount of correct classifications of naphthalene is 86 % for sensor PLD-8e-2 and above 99 % for sensor PLD-2e-1. Sensor PLD-2e-1 shows

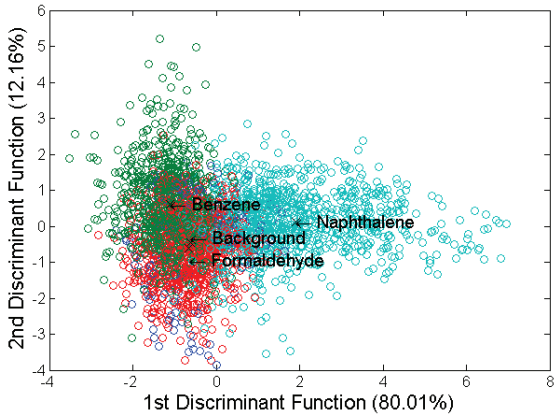

Fig. 5: Plot of LDA result (Ansatz A1) for sensor PLD-8e-2 (0.08 mbar O_2 partial pressure)

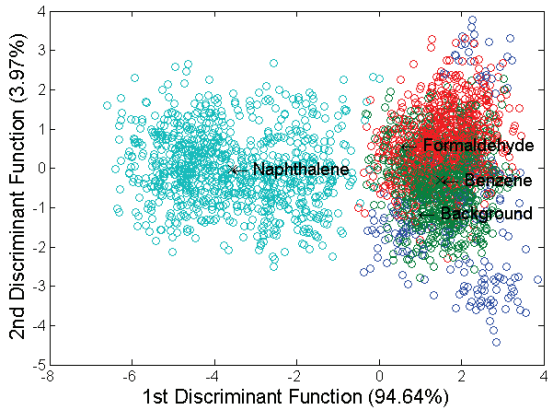

Fig. 7: Plot of LDA result (Ansatz A1) for sensor PLD-2e-1 (0.2 mbar O_2 partial pressure)

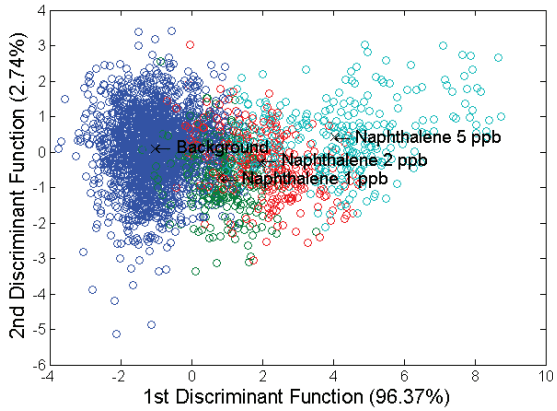

Fig. 8: Plot of LDA result (Ansatz A2) for sensor PLD-8e-2 (0.08 mbar O_2 partial pressure)

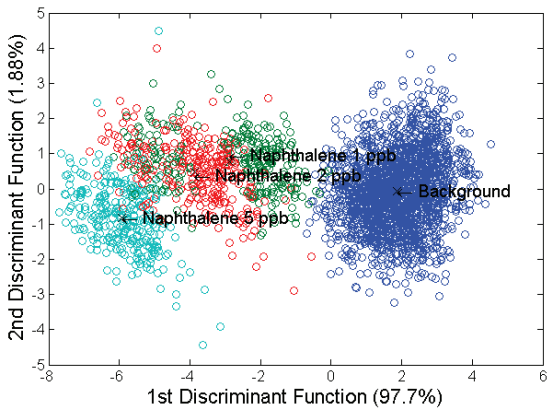

Fig. 9: Plot of LDA result (Ansatz A2) for sensor PLD-2e-1 (0.2 mbar O_2 partial pressure)

better performance for identifying the gases. Sensor PLD-8e-2 has very poor results especially for discriminating the data without VOC trace gases ("Background") from the trace VOCs: only 10.8 % of the "Background" data points are classified correctly, compared to 48.6 % for the second sensor.

Based on the results of the first LDA data evaluation, a quantification of naphthalene was attempted ("Ansatz A2"). For this, the three naphthalene concentrations were assigned to separate groups, still containing all RH levels and ethanol backgrounds. The TCO data sets of the other target VOCs (benzene, formaldehyde) were added to the background group.

The plots of the LDA results are shown in Fig. 8 for Sensor PLD-8e-2 and in Fig. 9 for PLD-2e-1. For both sensors, there is a separation of the naphthalene concentrations along the first discriminant function (green 1 ppb, red 2 ppb, light blue 5 ppb). As in the previous evaluation, the discrimination looks better for sensor PLD-2e-1, especially the separation of the low concentration data points from the background group (dark blue). The separation of the naphthalene groups from one another is not very distinct, especially for the PLD-8e-2 sensor. In the plot of the result of the PLD-2e-1 sensor, there are a number of "1 ppb" points that are located within the "2 ppb" group. Detailed analysis shows that these data points represent sensor signals recorded while no ethanol background was present, independent of gas humidity. This is probably a result of the LDA data processing, as the raw data values do not differ much for the two lowest concentrations, especially without ethanol background. With the interferent, the sensor data value range is more stretched within a temperature cycle.

Table 3 shows the validation results using LOOCV.

Table 3: LOOCV results for LDA of both sensors, Ansatz A2

Group	Correctly classified data points [%], Ansatz A2	
	PLD-8e-2	PLD-2e-1
Overall	83.3512	94.0336
Background	95.8742	99.8969
Naphthalene 1 ppb	42.7083	74.3056
Naphthalene 2 ppb	48.5915	73.2394
Naphthalene 5 ppb	73.9583	94.7917

Sensor PLD-2e-1 shows significantly better classification for all groups, especially for the low and medium naphthalene concentrations. Nearly 100 % of the background data sets are classified correctly, so there are almost no "false positive" classifications for naphthalene. However, the discrimination of the WHO guideline value (2 ppb) from lower concentrations needs to be improved for the application of demand controlled ventilation.

Conclusion

Nanostructured WO_3 layers have been prepared using pulsed laser deposition. The structure of the deposited material depends on the oxygen partial pressure applied during deposition. The size of agglomerations of nanoparticles can be changed with this parameter.

The differences in morphology of the two variants of the material are also reflected in their gas detecting performance. Both sensors react very well to ppb levels of naphthalene compared to the other tested VOCs, but the

sensor prepared with higher oxygen partial pressure (0.2 mbar) shows superior selectivity and sensitivity to naphthalene. Despite the changing and high ethanol background (factor 1000 between lowest naphthalene concentration and highest ethanol concentration), naphthalene can be identified in over 99 % of the respective data sets using the TCO sensor signals and linear discriminant analysis. A quantification is also possible with the PLD-2e-1 sensor but with poor accuracy for the low concentrations. Only for the highest naphthalene concentration (5 ppb) the LOOCV shows an acceptable classification result.

The measurement results indicate that the ε-phase of the gas sensitive WO_3 layer has significant impact on the gas sensing performance.

WO_3 layers prepared by PLD seem to be a very promising material for selective detection of naphthalene but for a reliable detection of the limit value their performance needs to be improved further; this includes optimization of the process parameters as well as the temperature cycle and the data processing for the specific sensors.

Acknowledgement

This project has received funding from the European Union's Seventh Framework Programme for research, technological development and demonstration under grant agreement No 604311, Project SENSIndoor.

References

[1] World Health Organization: WHO Guidelines for Indoor Air Quality: Selected Pollutants, Geneva (2010)

[2] J. Huotari, J. Lappalainen, J. Puustinen, A. Lloyd Spetz, Gas Sensing Properties of Pulsed Laser Deposited Vanadium Oxide Thin Films with Various Crystal Structures, *Sensors and Actuators B: Chemical* 187, 386-394 (2013); doi: 10.1016/j.snb.2012.12.067

[3] M. K. Verma, V. Gupta, A Highly Sensitive Sno_2–Cuo Multilayered Sensor Structure for Detection of H_2S Gas, *Sensors and Actuators B: Chemical* 166-167, 378-385 (2012); doi: 10.1016/j.snb.2012.02.076

[4] R.F. Wood, J.N. Leboeuf, K.R. Chen, D.B. Geohegan, A.A. Puretzky, Dynamics of Plume Propagation, Splitting, and Nanoparticle Formation During Pulsed-Laser Ablation, *Applied Surface Science* 127-129, 151-158 (1998); doi: 10.1016/S0169-4332(97)00625-9

[5] M. Leidinger, T. Sauerwald, W. Reimringer, G. Ventura, and A. Schütze, Selective detection of hazardous VOCs for indoor air quality applications using a virtual gas sensor array, J. Sens. Sens. Syst., 3 (2014), pp. 253-263, doi:10.5194/jsss-3-253-2014

[6] Martin Leidinger, Tilman Sauerwald, Andreas Schütze, Optimierter dynamischer Betrieb und multivariate Signalauswertung zum selektiven Nachweis von VOC im ppb-Bereich, 17. ITG / GMA Fachtagung 2014, ITG Fachbericht 250, VDE Verlag, 2014, ISBN 978-0-8007-3622-5

[7] C. Bur, P. Reimann, M. Andersson, A. Schütze, A.L. Spetz: Increasing the Selectivity of Pt-Gate SiC Field Effect Gas Sensors by Dynamic Temperature Modulation, IEEE Sensors Journal, Vol. 12, Iss. 6, pp: 1906 - 1913; doi: 10.1109/JSEN.2011.2179645

[8] D. Puglisi, J. Eriksson, C. Bur, A. Schuetze, A. Lloyd Spetz, M. Andersson: Catalytic metal-gate field effect transistors based on SiC for indoor air quality control, J. Sens. Sens. Syst., 4 (2015), pp. 1-8, doi: 10.5194/jsss-4-1-2015

[9] M. B. Johansson, G. A. Niklasson, L. Österlund, Structural and Optical Properties of Visible Active Photocatalytic WO_3 Thin Films Prepared by Reactive DC Magnetron Sputtering, *Journal of Materials Research* 27, 3130-3140 (2012); doi: 10.1557/jmr.2012.384

[10] B. Marinkovic, R. Ribeiro de Avillez, A.Saavedra, F. C. R. Assunção, A comparison between the Warren-Averbach method and alternate methods for x-ray diffraction microstructure analysis of polycrystalline specimens, *Materials Research*, 4 71-76 (2001); doi; 10.1590/S1516-14392001000200005.

[11] N. Helwig, M. Schüler, C. Bur, A. Schütze and T. Sauerwald, "Gas mixing apparatus for automated gas sensor characterization", 2014 Meas. Sci. Technol. 25 055903; doi: doi:10.1088/0957-0233/25/5/055903

[12] A.P. Lee, B.J. Reedy, „Temperature modulation in semiconductor gas sensing", Sensors and Actuators B 60 (1999), pp. 35-42

[13] Gutierrez-Osuna, R.: Pattern Analysis for machine olfaction: A review, IEEE Sens. Journal, 2 (3) (2002), pp. 189-202. doi: 10.1109/JSEN.2002.800688

[14] Bur, C., Bastuck, M., Lloyd Spetz, A., Andersson, M. and Schütze, A.: Selectivity enhancement of SiC-FET gas sensors by combining temperature and gate bias cycled operation using multivariate statistics, Sensors & Actuators B 193 (2014), pp. 931-940, doi: 10.1016/j.snb.2013.12.030.